2-бөлім **Раздел 2** **Section 2**

Қолданбалы математика **Прикладная математика** **Applied mathematics**

IRSTI 30.17.27 DOI: https://doi.org/10.26577/JMMCS202512848

D. B. Zhakebayev[1,2], **Y. Bakytbek**[3], **K. K. Karzhaubayev**[1,2*]
[1] Al-Farabi Kazakh National University, Almaty, Kazakhstan
[2] National Engineering Academy of Republic of Kazakhstan, Almaty, Kazakhstan
[3] Nazarbayev Intellectual school of Science and Mathematics, Almaty, Kazakhstan
*e-mail: kairzhan.k@gmail.com

NUMERICAL SIMULATION OF DECAYING TURBULENCE IN THE PRESENCE OF FREELY MOVING BUOYANT SOLID PARTICLES OF FINITE-SIZE

We present interface-resolved direct numerical simulations of decaying homogeneous isotropic turbulence laden with finite-size spherical particles. The fluid phase is solved using the lattice Boltzmann method (LBM) coupled with the interpolated bounce-back (IBB) scheme to impose no-slip boundary conditions at moving particle surfaces. The accuracy of the method is verified against benchmark cases, including the settling sphere experiment of ten Cate et al. and pseudo-spectral simulations of single-phase turbulence. Simulations are performed at an initial Taylor-scale Reynolds number in the range of $Re_\lambda = 20 - 45$ for particle volume fraction of 2.5%. The results show that finite-size particles enhance small-scale flow structures and accelerate the decay of turbulent kinetic energy compared to the single-phase case. Energy spectra analysis reveals a redistribution of energy from large to small scales. These findings provide new insights into turbulence modulation mechanisms in particle-laden flows and demonstrate the applicability of LBM for fully resolved particle–turbulence interaction studies.
Keywords: particle-laden, turbulence, multiphase, LBM, DNS.

Д. Б. Жакебаев[1,2], Е. Бақытбек[3], К. К. Каржаубаев[1*]
[1] Қазақстан Республикасының Ұлттық Инженерлік Академиясы, Алматы, Қазақстан
[2] Әл-Фараби атындағы Қазақ Ұлттық Университеті, Алматы, Қазақстан
[3] Назарбаев Зияткерлік Мектебі, Алматы, Қазақстан
*e-mail: kairzhan.k@gmail.com

Шекті өлшемдегі еркін қозғалатын қалқымалы қатты бөлшектердің қатысуымен ыдырайтын турбуленттікті сандық модельдеу

Осы жұмыста біз шекті өлшемді сферикалық бөлшектермен жүктелген ыдырайтын біртекті изотропты турбуленттіліктің тікелей сандық модельдеу нәтижелерін ұсынамыз. Сұйық фазаның динамикасы торлы Больцман әдісімен (LBM) шешіледі, ол қозғалыстағы бөлшектер бетінде жабысып тұру шекаралық шарттарын қою үшін интерполяцияланған шағылысу (IBB) сұлбасы қолданылған. Әдістің дәлдігі сынақтық есептерде тексерілді, соның ішінде сфералық бөлшектің шөгу тәжірибесімен және бірфазалы турбуленттілікке арналған псевдоспектралды әдіс нәтижелерімен салыстыру орындалды. Есептеулер Тейлор масштабы бойынша бастапқы Рейнольдс сандарының мәні $Re_\lambda = 20-45$ диапазонында болғанда және бөлшектердің көлемдік үлесі 2.5% кезінде жүргізілді. Нәтижелер бөлшектердің шекті өлшемдері ағынның ұсақмасштабты құрылымдарын күшейтіп, турбуленттік кинетикалық энергияның бірфазалы жағдаймен салыстырғанда тезірек өшуін жеделдететінін көрсетті. Энергетикалық спектрлерді талдау энергияның үлкен масштабтардан кіші масштабтарға ауысуын айқындады. Бұл нәтижелер бөлшектер бар ағындардағы турбуленттілікті модуляциялау механизмдері туралы жаңа мәліметтер береді және «бөлшек–турбуленттілік» өзара әрекеттесуін толық шешілетін зерттеулерге LBM әдісінің қолданбалығын көрсетеді.
Түйін сөздер: батырылған бөлшектер, турбуленттілік, көп фазалық ағындар, LBM, DNS.

Д. Б. Жакебаев[1,2], Е. Бақытбек[3], К.К. Каржаубаев[1*]
[1] Национальная Инженерная Академия Республики Казахстан, Алматы, Казахстан
[2] Казахский национальный университет имени аль-Фараби, Алматы, Казахстан
[3] Назарбаев Интеллектуальная Школа, Алматы, Казахстан
*e-mail: kairzhan.k@gmail.com

Численное моделирование затухающей турбулентности в присутствии свободно движущихся плавучих твердых частиц конечного размера

В данной работе нами представлены результаты прямого численного моделирования затухающей изотропной однородной турбулентности нагруженной сферическими частицами конечного размера. Динамика жидкой фазы разрешается методом решётчатого Больцмана (LBM), совмещённой с интерполированной схемой отражения (IBB) для задания граничных условий прилипания на поверхностях движущихся частиц. Точность метода подтверждается на тестовых задачах, включая эксперимент по оседанию сферы и при сравнении с результатами псевдоспектрального метода для однофазной турбулентности. Расчёты выполнены при начальных числах Рейнольдса по масштабу Тейлора в диапазоне $Re_\lambda = 20-45$ при объёмной доле частиц 2.5%. Результаты показывают, что частицы конечного размера усиливают мелкомасштабные структуры течения и ускоряют затухание турбулентной кинетической энергии по сравнению с однофазным случаем. Анализ энергетических спектров выявляет перераспределение энергии от больших к малым масштабам. Эти результаты предоставляют новые сведения о механизмах модуляции турбулентности в потоках с частицами и демонстрируют применимость LBM для полностью разрешённых исследований взаимодействия частицы–турбулентность.
Ключевые слова: погруженные частицы, турбулентность, многофазные течения, LBM, DNS.

1 Introduction

Turbulence laden with solid particles is a phenomenon of fundamental and practical importance in a wide range of natural and industrial processes, including sediment transport, atmospheric dust dynamics, spray combustion, and chemical mixing. Understanding the dynamics of such flows is particularly challenging due to the complex interplay between turbulent eddies and dispersed particles, especially when the particles are of finite size and can modulate the turbulence field [2].

Recent advances in numerical analysis, and computing hardware allowed researchers to gain more knowledge about two-way interactions of the flow and dispersed solid phase through interface-resolved direct numerical simulations (DNS), where all the flow details around moving solid particles are explicitly resolved, without a need to rely to empirical models or assumptions. The configuration of the turbulent flows in such studies is often described by the decaying homogeneous isotropic turbulence (DHIT) case, which offers a simple environment without of mean shear, wall effects, and external forcing. It enables the isolation and detailed examination of turbulence modulation mechanisms induced by particles, including attenuation or enhancement of turbulent kinetic energy (TKE), spectral energy redistribution, and modifications of small-scale intermittency.

[15] presented particle-resolved direct numerical simulations of homogeneous isotropic turbulence containing small, fixed spheres to investigate their impact on turbulence structure and decay. By resolving the flow around each sphere, detailed near-field and wake dynamics were captured which were absent in point-particle models[4]. The results show that the presence of fixed particles enhances small-scale dissipation and alters the energy spectrum, leading to increased energy at smaller scales and a faster decay of turbulent kinetic energy. The study further demonstrates that wake-induced fluctuations are a dominant mechanism for turbulence modification and provides quantitative measures of the additional dissipation generated by particle wakes.

One of the recent works by [12] employed direct numerical simulations of finite-size spherical particles in decaying homogeneous isotropic turbulence, focusing on particle-induced modulation of turbulence and the underlying mechanisms. The results show that particles generally enhance small-scale dissipation and alter the decay rate of turbulent kinetic energy, with the effect depending on particle size relative to the Kolmogorov length scale and the solid volume fraction. Energy spectra reveal a transfer of energy from large to small scales in the presence of particles. The study also quantifies additional dissipation from particle wakes and demonstrates that particle Reynolds number and wake dynamics play a central role in modifying turbulence decay.

Oka and Goto [9] investigated the attenuation of turbulence in a periodic cube by finite-size spherical solid particles through direct numerical simulations using an immersed boundary method to resolve flow around each particle, with fixed volume fraction $\phi = 8.2 \times 10^{-3}$ and systematically varying particle diameters d and Stokes numbers St. They found that turbulent kinetic energy attenuation is governed by the additional energy dissipation rate ϵ_p in particle wakes. Based on their simulation results authors proposed conditions for turbulence attenuation by finite-size particles.

While previous works incorporated discretized form of the Navier-Stokes equations to solve for the motion of the fluids [7], [5] used the Lattice Boltzmann Method (LBM) as fluid solver, combined with the interpolated bounce-back (IBB) boundary scheme to account for dynamic fluid-solid interface. The authors demonstrated that such numerical method can archive second order spatial accuracy and good computational efficiency, proposing its usage for turbulent flows laden with finite-size particles.

From the above mentioned examples, it is evident that the study of detailed mechanisms of turbulence decay in the presence of finite-size particles remain an active research area. Presence of the finite-size particles can significantly affect the temporal decay of turbulence. These effects depend strongly on several dimensionless parameters, such as the particle Stokes number, volume fraction, density ratio, and Reynolds number. In particular, when the particles are large compared to the Kolmogorov length scale, the interaction becomes two-way or even four-way coupled, involving significant feedback from particles to the fluid and particle-particle interactions [2].

In this study, we perform interface-resolved DNS of decaying particle-laden turbulence using the LBM method with fully resolved flow around spherical solid particles. Our aim is to investigate the effect of finite-size particles on the decay of turbulence at different flow Reynolds numbers, along this way we also demonstrate that kinetic methods, such as LBM are suitable for such complex cases as particle-laden turbulent flows. In the next section we provide the details of the combined LBM-IBB method we use, followed by Section 3, where validation cases and simulation results for particle-laden DHIT problem cases are presented. Finally, in the end we present conclusions to this work.

2 Numerical Methods

In this section the numerical methods used to simulate fluid and solid (dispersed) phases are described, including the details of the particle-particle collision treatment and scheme to enforce a no-slip boundary condition on the surface of the freely moving finite-size particles.

2.1 Lattice Boltzmann Method for Fluid Flow

The fluid motion is simulated using the Lattice Boltzmann Method, a kinetic approach that solves the discrete Boltzmann equation on a cubic mesh. We employ the three-dimensional, 27-velocity lattice model (D3Q27, see Fig. 2.1) , where the evolution of the particle distribution function $f_i(\mathbf{x}, t)$ is governed by the lattice Boltzmann equation with the Bhatnagar-Gross-Krook (BGK) approximation:

$$f_i(\mathbf{x} + \mathbf{c}_i\delta t, t + \delta t) = f_i(\mathbf{x}, t) - \frac{1}{\tau}\left(f_i(\mathbf{x}, t) - f_i^{\text{eq}}(\mathbf{x}, t)\right), \tag{1}$$

where $\mathbf{c}_i$ is the discrete velocity in the i-th direction, τ is the relaxation time, δt is the timestep ($\delta t = 1$ in present work) and f_i^{eq} is the equilibrium distribution function given by:

$$f_i^{\text{eq}} = w_i\rho\left(1 + \frac{\mathbf{c}_i \cdot \mathbf{u}}{c_s^2} + \frac{(\mathbf{c}_i \cdot \mathbf{u})^2}{2c_s^4} - \frac{\mathbf{u} \cdot \mathbf{u}}{2c_s^2}\right), \tag{2}$$

where w_i are the lattice weights, ρ is the fluid density, $\mathbf{u}$ is the macroscopic velocity, and c_s is the lattice speed of sound. The D3Q27 discrete velocity model is utilized because it is found to be more accurate and stable for turbulent flows in complex configurations [13].

The macroscopic flow variables are recovered via the moments of the discrete disctribution function:

$$\rho = \sum_{i=0}^{26} f_i, \qquad \rho\mathbf{u} = \sum_{i=0}^{26} f_i\mathbf{c}_i. \tag{3}$$

The kinematic viscosity ν is related to the relaxation time τ through:

$$\nu = c_s^2\left(\tau - \frac{1}{2}\right)\delta t. \tag{4}$$

During numerical simulations, it is common to advance Eq. (1) in two step procedure consisting of *collision* and *streaming* steps.

Collision:

$$f_i^*(\mathbf{x}, t) = f_i(\mathbf{x}, t) - \frac{\delta t}{\tau}\left[f_i(\mathbf{x}, t) - f_i^{\text{eq}}(\rho, \mathbf{u})\right], \tag{5}$$

Streaming:

$$f_i(\mathbf{x} + \mathbf{c}_i\delta t, t + \delta t) = f_i^*(\mathbf{x}, t), \tag{6}$$

where f_i^* is the post-collision distribution function, and δt is the time step size.

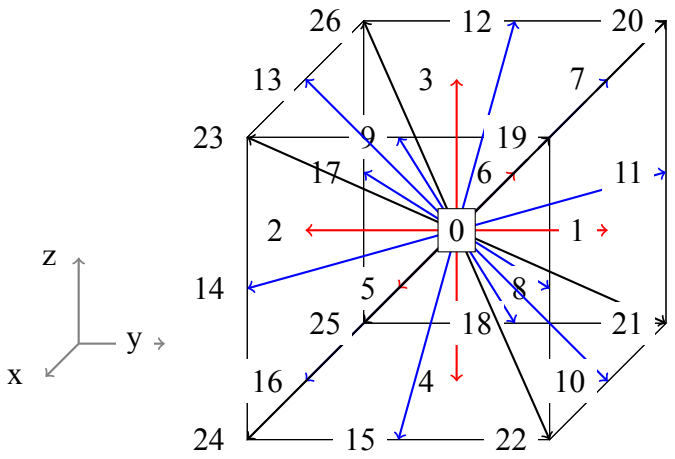

Figure 1: The D3Q27 discrete velocity model is used in the current work. The fluid particles are allowed to move only in the shown discrete directions. The cube centered at the origin $(0, 0, 0)$ has side length of 1.

2.2 Interpolated Bounce-Back Scheme for Moving Boundaries

The standard bounce-back scheme is a popular choice to enforce no-slip boundary condition in kinetic methods, such as LBM. However, it assumes that solid boundary is always located exactly half-way between fluid nodes. An improvement made by Bouzidi et al. [1] allowed to use bounce-back scheme on curvilinear boundaries with arbitrary location of solid boundary relative to fluid nodes. The key point in the improvement of Bouzidi et al. [1] is to use linear or quadratic interpolation to recover unknown fluid particles coming from the boundary. The interpolated bounce-back scheme is found to posses second-order of accuracy and is a common choice in laminar and turbulent flow simulations.

The idea behind IBB is demonstrated using one-dimensional example in Fig. 2. When a lattice link between a fluid node (x_f) and a solid node (x_b) intersects the particle boundary, the IBB scheme determines the exact intersection point and computes parameter q. The value of q defines which of two ways is used to recover unknown distributoin function values, heading off the solid boundary (that is, moving in the right direction at node x_f). In case $q \leq 0.5$, the value of f_i is equal to the pre streaming value of f_i at the node x_i, while in the case $q > 0.5$, f_i at the near boundary node x_f is recovered using interpolation through the values at nodes x_{fff}, x_{ff} and x_i. The required values at the node x_i also found using the interpolation.

The hydrodynamic force and torque acting on a particle are computed from the momentum exchange (Peng et al. [10]) at each fluid-solid interface:

$$\mathbf{F}_{\text{hydro}} = \sum_{x_f} \sum_{i} \Delta \mathbf{p}, \qquad \mathbf{T}_{\text{hydro}} = \sum (\mathbf{r} - \mathbf{r}_c) \times \Delta \mathbf{p}, \tag{7}$$

where particle nature of LBM is exploited, and $\Delta \mathbf{p}$ is the momentum exchanged across a lattice link, $\Delta \mathbf{p} = \left(\tilde{f}_i^t + f_{\bar{i}}^{t+\Delta t} \right) \cdot \mathbf{c}_i$, $\mathbf{r}_c$ is the center of the particle, and the summation extends over all links intersecting the particle surface.

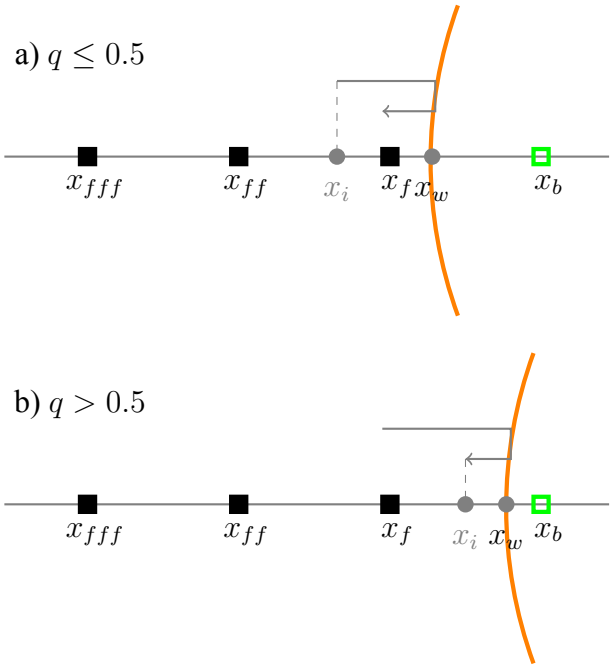

Figure 2: An example of the interpolated bounce-back scheme for two possible cases, depending on the parameter q which defines relative solid boundary intersection with velocity links, defined as $q = (x_w - x_f)/(x_b - x_f)$: a) $q \leq 0.5$, the unknown fluid particles are coming from the node x_i, b) $q > 0.5$, the unknown fluid particles ar node x_f are reconstructed from the data from the nodes x_{fff}, x_{ff} and x_i.

2.3 Particle Motion and Coupling

Particles are modeled as rigid spheres, and their motion is governed by the Newton-Euler equations:

$$m_p \frac{d\mathbf{u}_p}{dt} = \mathbf{F}_{\text{hydro}} + \mathbf{F}_{\text{coll}}, \tag{8}$$

$$\mathbf{I}_p \frac{d\boldsymbol{\omega}_p}{dt} = \mathbf{T}_{\text{hydro}} + \mathbf{T}_{\text{coll}}, \tag{9}$$

where m_p and $\mathbf{I}_p$ are the particle mass and moment of inertia, $\mathbf{u}_p$ and $\boldsymbol{\omega}_p$ are the translational and angular velocities of the particle, and $\mathbf{F}$, $\mathbf{T}$ represent forces and torques acting on a particle due to interaction with the surrounding fluid (subscript hydro) and collision with other particles (subscript coll).

The fluid-particle interaction is resolved at each time step. First, the LBM updates the fluid flow field (Eqs. (5, 6)), after which hydrodynamic forces and torques are computed via the IBB scheme. The particle motion is then integrated based on the computed forces, and updated positions and velocities are used in the next iteration of the IBB scheme. Eqs. (8, 9) are discretized using second-order scheme.

2.4 Collision and Lubrication Modeling

To account for short-range hydrodynamic interactions (Fig. 3) that are under-resolved on the lattice, particularly during close particle-particle approaches, a lubrication correction model is employed. Specifically, a soft-sphere collision model with linear spring-dashpot mechanics combined with a lubrication force correction is employed in this work. This approach provides physically correct contact mechanics and helps to avoid nonphysical particle overlapping.

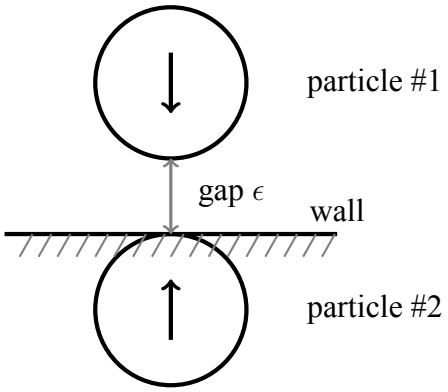

Figure 3: An example of particle-particle or particle-wall interaction. The gap between particles or between particle and wall is denoted as ϵ.

The particle interaction force is split into two constituents $\boldsymbol{F}_{coll} = \boldsymbol{F}_l + \boldsymbol{F}_s$, $\boldsymbol{F}_l$ accounts for lubrication correction and $\boldsymbol{F}_s$ for soft-sphere collision. The magnitude of $\boldsymbol{F}_l$ is then:

$$F_l(\epsilon, u_n) = -6\pi\mu_f R u_n[\lambda(\epsilon) - \lambda(\epsilon_{sw})], \tag{10}$$

where u_n - relative velocity, ϵ - gap width, and ϵ_{sw} is the distance at which correction is activated. The particular forms for λ depend on the type of interaction, analytical forms of which were given by Brenner [3], and for particle-particle interactions $\lambda = \lambda_{pp}$:

$$\lambda_{pp} = \frac{1}{2\epsilon} - \frac{9}{20} ln(\epsilon) - \frac{3}{56}\epsilon ln(\epsilon) + 1.346 + \mathcal{O}(\epsilon). \tag{11}$$

The soft-sphere contact collision force takes the form of a spring-dashpot system with the magnitude of $\boldsymbol{F}_s$ given as:

$$F_s = -k_n\delta - \beta_n u_n \tag{12}$$

where k_n is the spring stiffness parameter, β_n is the dashpot resistance parameter and $t = N_c\Delta t$ - collision time:

$$k_n = -\frac{m_e(\pi^2 + [\ln e_d]^2)}{[N_c\Delta t]^2}, \beta_n = -\frac{2m_e[\ln e_d]}{[N_c\Delta t]}. \tag{13}$$

The coefficients k_n and β_n are the functions of the collision time $t = N_c\Delta t$, effective mass m_e and of the coefficient of dry restitution. They form spring-dashpot system and guarantee that particle re-bounces during the collision with duration of $t = N_c\Delta t$ with the velocity $u_c^* = e_d u_c$, where u^* is the velocity at the end of the contact interaction.

3 Simulation results

As a validation of the code first the single-phase Decaying Homogeneous Isotropic Turbulence (DHIT) problem was compared to spectral simulation results. For this case, Rogallo's procedure [11] was used to generate an initial divergence-free velocity field with the prescribed energy spectrum. The initial energy spectrum is given by [16]

$$E_0(k) = Ak^4 e^{-0.14k^2},$$

with energy containing wavenumbers $k = [k_a, k_b] = [3, 8]$ and coefficient $A = 1.1474 \times 10^{-2}$. The flow is prescribed for the DHIT problem using the Taylor microscale-based Reynolds number Re_λ defined as

$$Re_\lambda = \frac{u_{rms}\lambda}{\nu},$$

where u_{rms} is *Root-Mean-Square* (RMS) velocity, λ is Taylor micro length scale, and ν is fluid kinematic viscosity.

The numerical simulation results for the evolution of turbulent kinetic energy and energy dissipation at $Re_\lambda = 26$, obtained from the LBM and the benchmark pseudo-spectral simulation [6], are presented in Fig. 4. The excellent agreement between the kinetic method and the pseudo-spectral simulation at a mesh resolution of 256^3 strongly supports the applicability of the LBM to turbulent flow simulations.

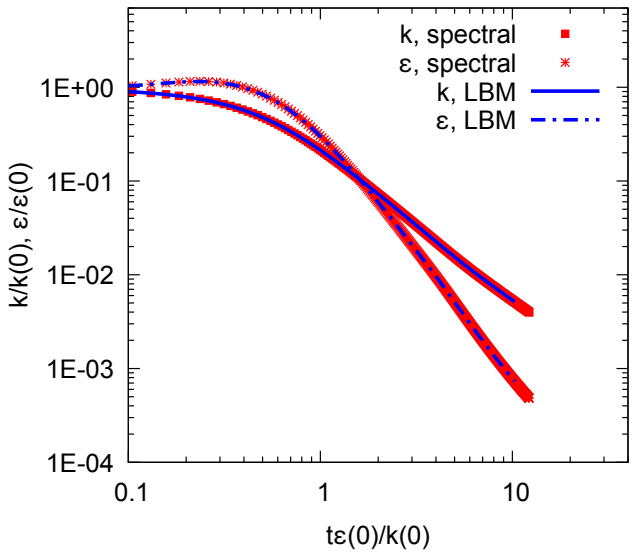

Figure 4: Evolution of the turbulent kinetic energy (k) and it's dissipation rate (ϵ) for DHIT problem.

To validate the accuracy of the numerical method for two-phase cases, we compare our simulation results with the experimental data reported by ten Cate et al. [8] for the solid particle settling problem. In their study, the motion of a single solid sphere settling under gravity in a quiescent viscous fluid was investigated using particle image velocimetry (PIV). The experiments were conducted in a square tank with dimensions $100 \times 100 \times 160\,\text{mm}^3$, and the diameter of

the sphere was $d = 15\,\text{mm}$. The sphere was released at the height of 120 mm above bottom of the tank and was allowed to settle freely. The fluid used was a water–glycerol mixture with varying viscosities, and the density ratio between the particle and fluid was in the range of $\rho_p/\rho_f = 1.15 - 1.16$. The Reynolds number based on terminal velocity ranged from $Re \approx 1.5$ to 32, covering both creeping and moderately inertial regimes. In Fig. 5 the evolution of the particle settling velocity is shown. Here, again very good agreement between numerical results from LBM and experimental data indicate sufficient validation and performance of the newly implemented kinetic approach.

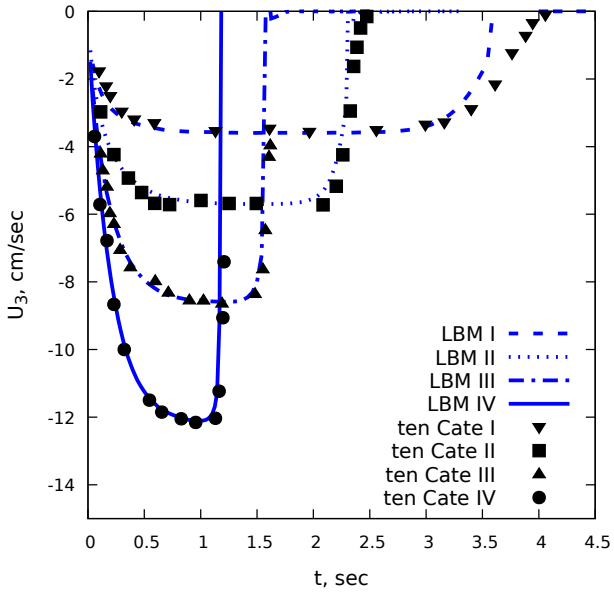

Figure 5: Evolution of the particle settling velocity compared with experimental data of cases I-IV from Ten Cate et al. [14].

After above mentioned validation cases we now present DHIT results for particle-laden and particle-free cases. In total six simulations were performed, three of which are single-phase cases and other three are particle-laden counterparts of fluid only cases. The carrier flow properties are shown in Table 1, whereas suspended solid phase properties are shown in Table 2.

#	L	N	k_0	u_{rms}	ν	Re_λ
I	256	256	$3.52 \cdot 10^{-4}$	$1.53209 \cdot 10^{-2}$	0.0121	20
II	256	256	$3.52 \cdot 10^{-4}$	$1.53209 \cdot 10^{-2}$	0.0101	30
III	256	256	$3.52 \cdot 10^{-4}$	$1.53209 \cdot 10^{-2}$	0.0068	45

Table 1: Fluid phase properties for single-phase and particle-laden cases.

The DHIT problem was defined in the cubic domain with periodic boundary conditions in all three directions with the length of the cube side as L and the mesh resolution of N. The initial kinetic energy of the flow is k_0, while RMS velocity of the initial flow is u_{rms}. Turbulence was characterized using the Taylor microscale Reynolds number Re_λ. In particle-laden cases the volume fraction of

#	N_p	ρ_p/ρ_f	ϕ	$d/\Delta x$	d/λ	d/η
I	50	1.0	2.5%	25.6	12.93	12.7
II	50	1.0	2.5%	25.6	12.93	13.91
III	50	1.0	2.5%	25.6	12.93	14.91

Table 2: Solid-phase properties for particle-laden counterparts of the single-phase flows shown in Table 1.

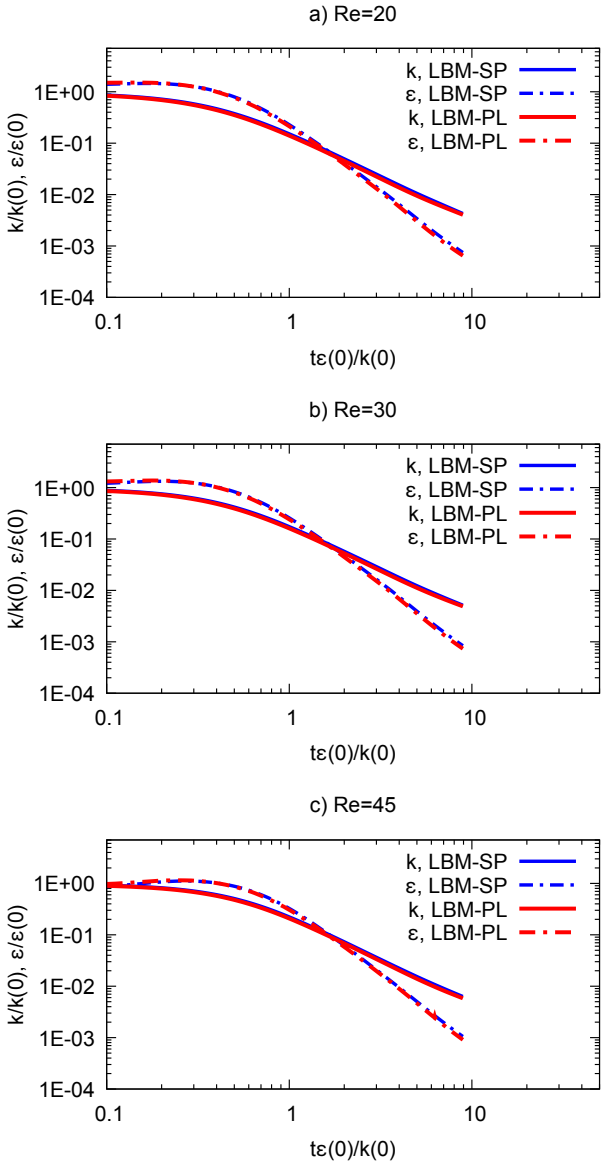

Figure 6: Evolution of the flow turbulent kinetic energy and dissipation rate for single-phase (SP) and particle-laden (PL) cases at different Reynolds numbers.

the solid-phase is set to 2.5% with the number of buoyant particles equal to 50. Particle diameter (d) and mesh resolution was large enough to allow properly resolve all flow scales, including Taylor (λ)

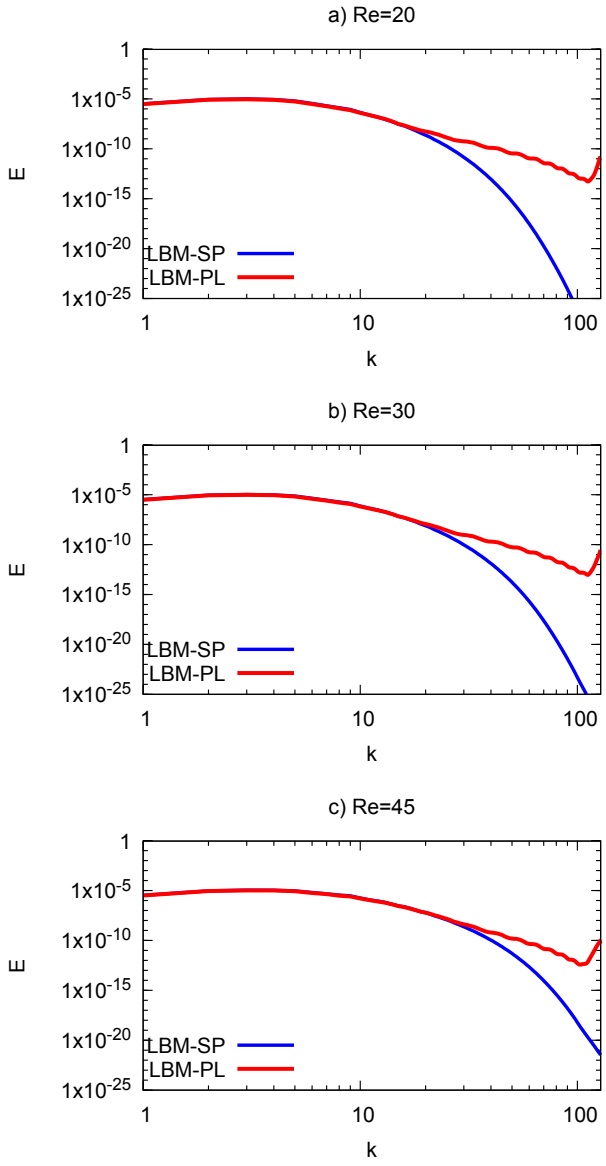

Figure 7: Comparison of turbulence energy spectra at $t^* = 1$ between single-phase (SP) and particle-laden cases (PL).

and Kolmogorov (η) length scales. Particle-laden cases were identical to single-phase cases, except that buoyant particles were introduced to the flow after one step of LBM algorithm.

Evolution of the flow turbulent kinetic energy and dissipation rate for single-phase and particle-laden cases at different Reynolds numbers are shown in Fig. 6. For all three considered cases which differ only in the initial flow Reynolds numbers, increase of dissipation rate due to the introduction of the particles is visible at the beginning of the simulation. However, at later time the energy dissipation rate becomes lower for PL cases. For all PL cases slight reduction of the TKE is observable. This decrease of TKE is usually related to enhanced energy dissipation at the surface of freely moving particles.

Overall, evolution of TKE and energy dissipation is quite close to the ones in the single-phase cases due to the relatively low volume fraction of suspended phase. At the same time, no significant Reynolds number dependence in the behavior of the energy evolution is visible.

Comparison of the turbulence energy spectra at non-dimensional time $t^* = 1$ between single-phase (SP) and particle-laden cases (PL) is shown in Fig. 7. Immediately two observations can be underlined. First, we see an increase in energy of the small structures in PL cases relative to SP cases, related to a high wavenumber part of the spectra for all three Reynolds number cases. Second, energy distribution at high wavenumber part of the spectra has noticeable wiggling, which is related to velocity discontinuity on the solid-phase boundaries. Such osccillations can be considered as numerical artifact and will be ignored here. Level of energy increase of small structures is larger for lower Reynolds number cases. This can be explained due to enhanced introduction of the smaller structures to the flow by fixed-size particles. At larger Reynolds numbers, the flow already contains such small strucutres, and their enhancement due to the freely moving particles is minor.

4 Conclusions

From the performed work we can conclude that kinetic method of LBM is an efficient tool to study turbulence in multiphase flows, particularly, for flows with freely moving suspended finite-size particles. The second-order accuracy and stability of LBM is well suited to perform direct numerical simulations of turbulent flows. The decaying homogeneous isotropic turbulence problem studied here in single-phase and particle-laden cases revealed that modulation of turbulence is present, visible from energy enhancement at higher end of spectra and decreased overall TKE. For all three Reynolds numbers considered, such behaviour lasts, indicating that, at least under considered Reynolds number range ($Re_\lambda = 20-45$) no significant Reynolds number dependence is visible. For future works we suggest to hold similar studies at wider range of flow and solid-phase parameters such as ones shown in Tables 1 and 2.

Acknowledgments

The authors were supported by the Ministry of Science and Higher Education of the Republic of Kazakhstan Grant No. AP19680366.

References

[1] Bouzidi, M., M. Firdaouss, and P. Lallemand (2001). Momentum transfer of a boltzmann-lattice fluid with boundaries. *Physics of fluids 13*(11), 3452–3459.

[2] Brandt, L. and F. Coletti (2022). Particle-laden turbulence: progress and perspectives. *Annual Review of Fluid Mechanics 54*(1), 159–189.

[3] Brenner, H. (1961). The slow motion of a sphere through a viscous fluid towards a plane surface. *Chemical engineering science 16*(3-4), 242–251.

[4] Ferrante, A. and S. Elghobashi (2003). On the physical mechanisms of two-way coupling in particle-laden isotropic turbulence. *Physics of fluids 15*(2), 315–329.

[5] Gao, H., H. Li, and L.-P. Wang (2013). Lattice boltzmann simulation of turbulent flow laden with finite-size particles. *Computers & Mathematics with Applications 65*(2), 194–210.

[6] Karzhaubayev, K., L.-P. Wang, and D. Zhakebayev (2022). An efficient parallel spectral code for 3D periodic flow simulations. *SoftwareX 20*, 101244.

[7] Maussumbekova, S. and A. Beketaeva (2024). Numerical modeling of thrombus formation dynamics with the rheological properties of blood. *International Journal of Mathematics and Physics 15*(2), 94–100.

[8] Maxey, M. R. and J. J. Riley (1983, 04). Equation of motion for a small rigid sphere in a nonuniform flow. *The Physics of Fluids 26*(4), 883–889.

[9] Oka, S. and S. Goto (2022). Attenuation of turbulence in a periodic cube by finite-size spherical solid particles. *Journal of Fluid Mechanics 949*, A45.

[10] Peng, C., Y. Teng, B. Hwang, Z. Guo, and L.-P. Wang (2016). Implementation issues and benchmarking of lattice boltzmann method for moving rigid particle simulations in a viscous flow. *Computers & Mathematics with Applications 72*(2), 349–374.

[11] Rogallo, R. S. (1981). *Numerical experiments in homogeneous turbulence*, Volume 81315. National Aeronautics and Space Administration.

[12] Schneiders, L., M. Meinke, and W. Schröder (2017). Direct particle–fluid simulation of kolmogorov-length-scale size particles in decaying isotropic turbulence. *Journal of Fluid Mechanics 819*, 188–227.

[13] Suga, K., Y. Kuwata, K. Takashima, and R. Chikasue (2015). A d3q27 multiple-relaxation-time lattice boltzmann method for turbulent flows. *Computers & Mathematics with Applications 69*(6), 518–529.

[14] Ten Cate, A., C. Nieuwstad, J. Derksen, and H. Van den Akker (2002). Particle imaging velocimetry experiments and lattice-boltzmann simulations on a single sphere settling under gravity. *Physics of Fluids 14*(11), 4012–4025.

[15] Vreman, A. (2016). Particle-resolved direct numerical simulation of homogeneous isotropic turbulence modified by small fixed spheres. *Journal of Fluid Mechanics 796*, 40–85.

[16] Wang, P., L.-P. Wang, and Z. Guo (2016). Comparison of the lattice Boltzmann equation and discrete unified gas-kinetic scheme methods for direct numerical simulation of decaying turbulent flows. *Physical Review E 94*(4), 043304.

Авторлар туралы:

Дәурен Жакебаев — PhD, әл-Фараби атындағы Қазақ ұлттық университетінің профессоры, Қазақстан Республикасының Ұлттық Инженерлік Академияның бас ғылыми қызметкері (Алматы, Қазақстан, e-mail: zhakebayev@kaznu.kz);

Елзада Бақытбек - Алматы қаласының Наурызбай ауданының Назарбаев зияткерлік мектебінің оқушысы (Алматы, Қазақстан, e-mail: elzadabakytbek@gmail.com);

Қайыржан Қаржаубаев — PhD, Қазақстан Республикасының Ұлттық Инженерлік Академияның аға ғылыми қызметкері, Алматы, Қазақстан (Алматы, Қазақстан, e-mail: kairzhan.k@gmail.com).

Информация об авторах:

Даурен Жакебаев — PhD, профессор, Казахский Национальный Университет имени аль-Фараби, главный научный сотрудник Национальной Инженерной Академии Республики Казахстан, (Алматы, Казахстан, e-mail: zhakebayev@kaznu.kz);

Елзада Бақытбек - ученица Назарбаев интеллектуальной школы Наурызбайского района города Алматы (Алматы, Казахстан, e-mail: elzadabakytbek@gmail.com);

Каиржан Каржаубаев — PhD, старший научный сотрудник Национальной Инженерной Академии Республики Казахстан (Алматы, Казахстан, e-mail: kairzhan.k@gmail.com).

Information about authors:

Dauren Zhakebayev - PhD, Professor of Al Farabi Kazakh National University, Leading Researcher of National Engineering Academy of Republic of Kazakhstan (Almaty, Kazakhstan, e-mail:zhakebayev@kaznu.kz);

Yelzada Bakytbek - student of Nazarbayev Intellectual school of Science and Mathematics in Almaty (Almaty, Kazakhstan, e-mail: elzadabakytbek@gmail.com);

Kairzhan Karzhaubayev - PhD, Senior Researcher of National Engineering Academy of Republic of Kazakhstan (Almaty, Kazakhstan, e-mail:kairzhan.k@gmail.com).

Received: August 19, 2025
Accepted: December 10, 2025